

## PRECISION ANALYTICAL UNDERWATER PHOTOGRAMMETRY

E. Dorrer

Institute for Photogrammetry and Cartography  
Munich Bundeswehr University

### ABSTRACT

The major phases of an operational APL program package developed within a pilot project for the determination of deformations of industrial underwater objects are described. The paper emphasizes the chosen analytical approach for a suitable numerical solution of the "refracto-collinearity equation" and spatial multi-media resection and intersection. Due to uncertainties inherent in a multi-media environment, program operation is dialogue-oriented and menu-driven, thus facilitating the detection of inconsistencies and systematic disturbances in the data. Preliminary results obtained under simulated operational conditions confirm the validity, accuracy and reliability of the approach. The solution is entirely based on APL as a modern time-saving and highly efficient program language.

### INTRODUCTION

Within a pilot project for the photogrammetric determination of industrial underwater objects subject to deformation from a known nominal design shape, our institute has been engaged in the primary data processing phase. The photogrammetric survey method had been chosen due to the very high accuracy requirements of 0.5 mm and less over a length of some 5 m, and short exposure to the object in a perilous environment. Besides the measurement of photo coordinates with a precision analytical stereoplotter this phase consisted primarily of the design, generation and testing of a computer program package capable of handling multi-media geometry. Although various investigators had found theoretical solutions to this interesting problem in the past, and developed suitable methodologies (see e.g. ZAAR, 1948; RINNER, 1948, 1969; HOEHLE, 1971; OKAMOTO and HOEHLE, 1972; TORLEGARD, 1974), no readily-applicable software could be detected for this particular task. The project's pilot character, uncertainties of the mathematical model, imponderables in both the deterministic and stochastic behaviour of the data, and limitations in the availability of programming personnel suggested the use of A P L as programming language. As interpretative language utilizing a compact notation almost synonymous to mathematical nomenclature, APL inherently has the advantage that the final program code can be generated at least five times faster than with any other known language, and that unavoidable program modifications are quickly performed (DORRER, 1982). It was decided to develop a menu-oriented program package based entirely on APL.

In order to achieve the desired accuracy a specially designed frame-work of some 40 control point markers was supposed to enclose the object during photographic exposure. Manufactured from highly resistant and stable carbon fiber rods, this rigid frame-work had to be calibrated photogrammetrically under normal, i.e. "dry" conditions prior to submersion into water. A self-calibration method as suggested by WESTER-EBBINGHAUS (1983) had been used, yielding RMSE values for the coordinates of 0.10, 0.16, 0.09 mm in the three coordinates X, Y, Z with respect to a frame-work based system. The metric camera used has been a UMK 10/1318 with Lamagon 8/100A installed in a specifically constructed underwater housing with planar front end glass plate. The housing can be remotely driven towards the object in order to obtain an as large photo scale as possible. Normally three photographs are supposed to be taken from three different positions under water.

PHOTOGRAMMETRIC MEASUREMENT

With usually three convergent photographs covering the interesting side of one object (see also Section 5), the measurements are performed stereoscopically for each of the three photopairs in an analytical stereoplotter PLANICOMP C100. In order to speed up photogrammetric observation, computer-controlled positioning is rigorously applied to the backward measurement set in the same photopair and to subsequent photographs that have been measured before. One set of measurements in a stereopair consists of first the fiducial marks, then the control points, again the fiducials, then all object points, finally again the fiducials. All points are measured a second time in reverse order in a second set. Properly marked, both sets containing some 400 point measurements with four coordinates each are then stored on "general" file.

Control point identification numbers are keyed in as seen from the photographs. Id numbers for the actual object points need not be entered if a specified sequence of observations is followed. Only different point types must be identified by known one-digit numbers. The actual point numbers are generated by program in WS EINLESEN (see Section 6). Besides again speeding up the measurement phase, this feature is rather operator-friendly. As first practical measurements have shown, one photopair can be completed in roughly four hours continuous observation.

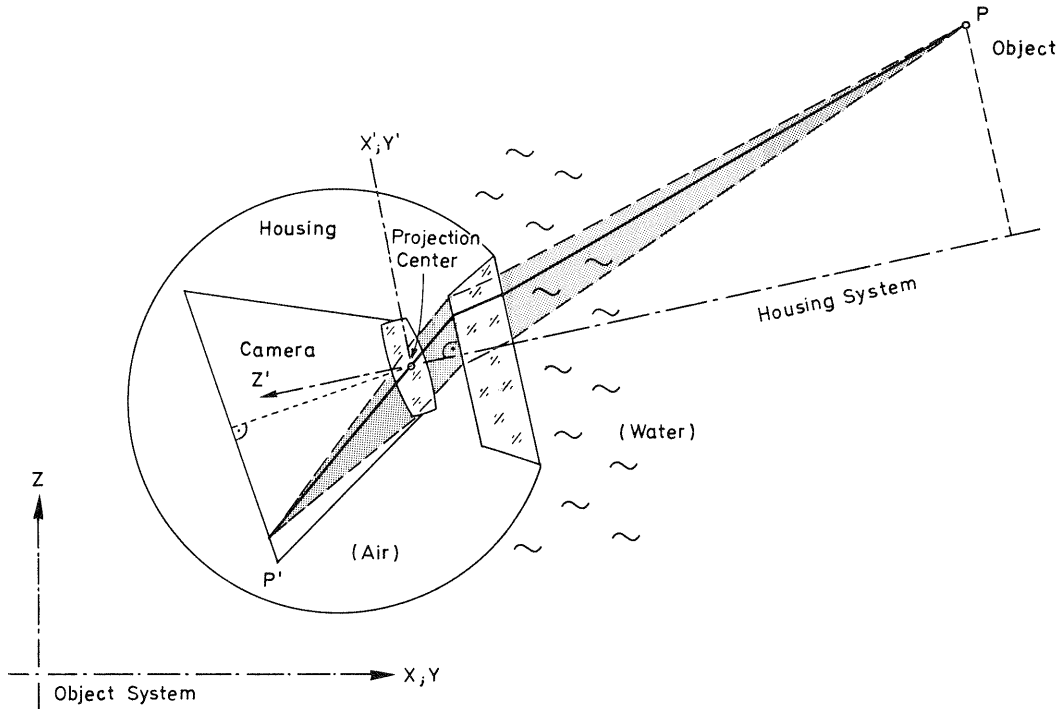


Figure 1. Special refracto-perspective imaging

REFRACTO-COLLINEARITY EQUATION

As indicated in fig. 1 the photogrammetric underwater image can be described by a special refracto-perspective mapping characterized by two or more parallel boundary planes between different optical media, e.g. air, water and several types of glass. Assuming a base system rigidly fixed to the housing as shown in fig. 1, the ray between an object point P and the perspective center C (fig. 2), intersecting the innermost boundary plane in an "image housing" point  $P_1$ , can be described by the radii,  $r_i$  and the distances,  $d_i$ ,  $i = 0, 1, \dots, g$  ( $g = \text{number of boundary planes}$ ). Due to this isotropy in the coordinates  $X_1$  and  $X_2$ ,  $r_0$  is representative for the "image housing" coordinates of  $P_1$ , from which actual image coordinates for the corresponding photo

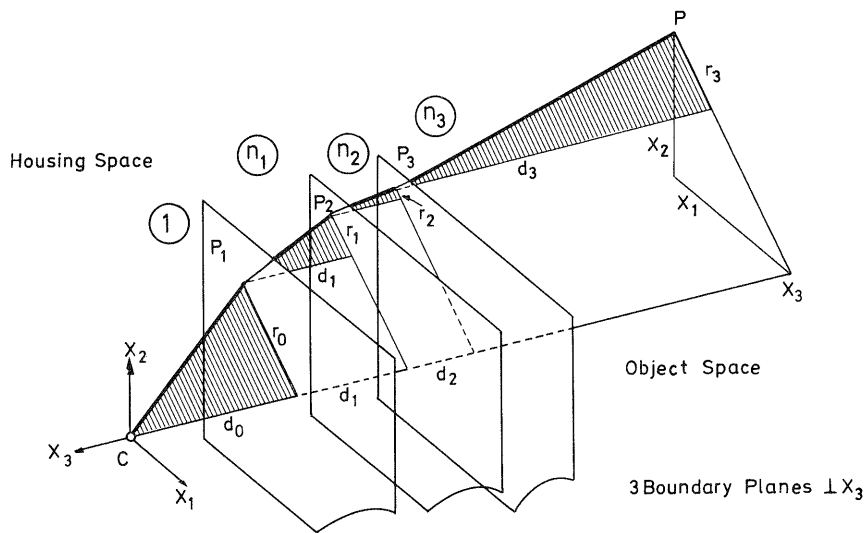


Figure 2. Isotropy of  $X_1, X_2$  and definition of "image housing" coordinates

point  $P'$  (fig. 1) can easily be derived. Denoting with  $D$  the distance between  $C$  and  $P$  along the  $X_3$ -axis, with  $R$  the normal distance from  $P$  to the  $X_3$ -axis, and with  $n_i$  the various refractive coefficients ( $n_0=0$ ), then the following equation (1) can be derived from Snell's law of refraction:

$$\rho_o = \frac{r_o}{d_o} = \frac{R}{d_o + \sum_{i=1}^g d_i \cdot \{n_i^2 + (n_i^2 - 1)\rho_o^2\}^{-1/2}}, \quad (1)$$

where

$$d_3 = D - \sum_{i=1}^g d_{i-1} \quad (2)$$

For given coordinates  $(R, D)$  of any object point  $P$ , and values for  $n_i, d_{i-1}, i = 1, 2, \dots, g$ , eqs. (1) and (2) can be used to determine normalized image housing coordinates  $\rho_o$  for the point  $P_1$ . Even in the simplest case with only one boundary plane ( $g=1$ ) between two refractive media, equ.(1) gives rise to an algebraic equation of 4th degree. All other configurations yield equations of higher degree for which no rigorous mathematical solution can be found. It was therefore decided to develop a fast algorithm for an iterative solution. Assuming  $g=1, r \ll R$  and  $d \ll D$ , a suitable initial approximation sufficiently close to  $\rho_o$  can be derived from equ.(1) yielding

$$\rho_o = \frac{n_g R}{\{D^2 - (n_g^2 - 1)R^2\}^{1/2}} \quad (3)$$

The APL-function *SRIM* shown in the appendix makes use of the aforementioned algorithm, and it must be considered as the fundamental application function for the special case of multi-media photogrammetry.

## RESECTION AND INTERSECTION

The number and distribution of the control points have been found sufficient for a distinct determination of the exterior orientation of each photograph (see also RINNER, 1948). Due to missing information on the exact refractive index of water at the time of exposure as well as on the orientation of the camera with respect to the

front end glass plate of the underwater housing, four additional parameters are introduced as part of the entire orientation. These parameters may be assumed constant during the photogrammetric survey of one object. Since modelling of systematic disturbances of the imaging geometry was considered rather difficult, particularly for the vertical gradient of the refractive index of water, it was decided to arrive at a suitable iterative solution by means of interaction with the human operator. The idea was extended to incorporating the aforementioned additional parameters as well. This has led to the flow diagram shown in fig. 3. After the input of all data per-

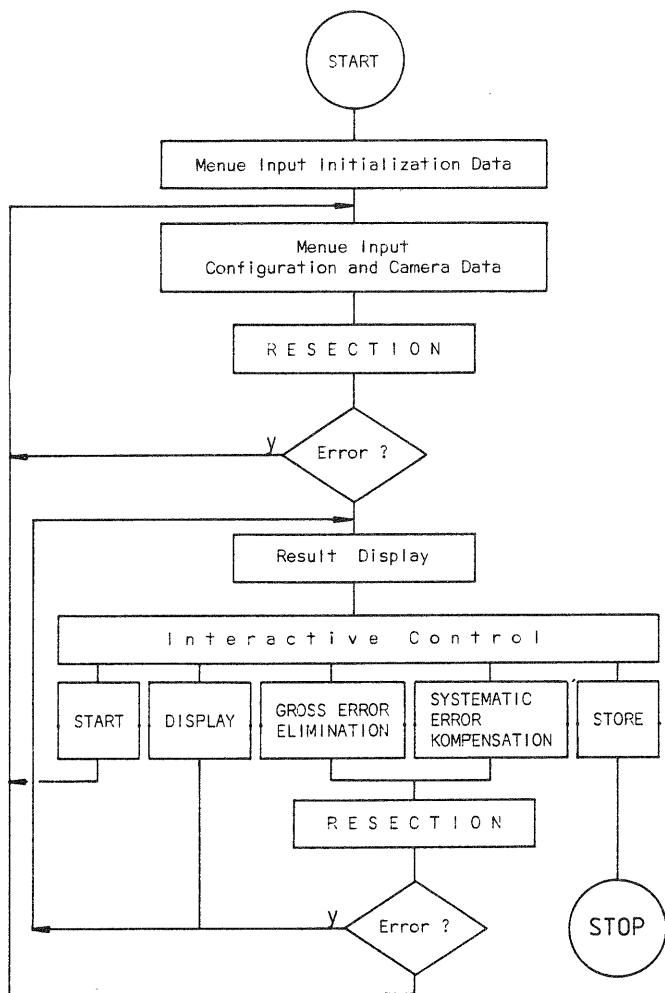


Figure 3.  
Flow diagram of RESECTION mode

tinent to a nonsingular solution of the numerical resection of two photographs — optionally several orientation parameters may be specified to be excluded from adjustment — the estimated results are displayed, viz. numerical values, plots and statistics of the residuals, orientation parameters with standard errors. By virtue of this display the operator has the choice to either eliminate specified control points, restart all computations or just have the results re-displayed, compensate for systematic errors or store the estimated data for subsequent processing. Although a posteriori compensation of systematic effects from the residuals of the image coordinates statistically is unsound, a properly organized re-adjustment nevertheless leads to reliable results.

Denoting the object coordinates of the control points by  $X$ , the corresponding image coordinates by  $x$ , the unknown (extended) orientation parameters by  $u$ , and the (differentially small) parameters describing systematic errors by  $ds$ , the following equation holds

$$x + T.ds + v = f(X,u) \quad , \quad ( 4 )$$

or in linearized form

$$dx + T.ds + v = A.du \quad (5)$$

The function  $f$  governs the refracto-collinearity relation between  $X$ ,  $u$  and  $x$ , while  $T$  is the coefficient matrix describing two bivariate polynomials. By neglecting the influence of  $ds$ , equ.(5) becomes

$$dx + v_o = A.du_o \quad (6)$$

yielding a preliminary least-squares solution

$$du_o = A^- . dx \quad , \quad (7)$$

where  $A^-$  stands for the pseudo-left inverse of  $A$ . This leads to the temporary residuals

$$v_o = -dx + A.du_o = (-I + A.A^-).dx \quad (8)$$

containing the deterministic part that now can be analysed interactively on the graphics screen. The operator is expected to control the degree of the polynomials by specifying the confidence interval of its estimated coefficients. In the solution

$$ds_o = T^- . v_o \quad (9)$$

only the significant coefficients are carried through. The final solution

$$\begin{aligned} ds &= (T - A.A^- . T)^- . v_o \\ du &= du_o + A^- . T.ds \end{aligned} \quad (10)$$

is identical to a simultaneous adjustment of equ.(5).

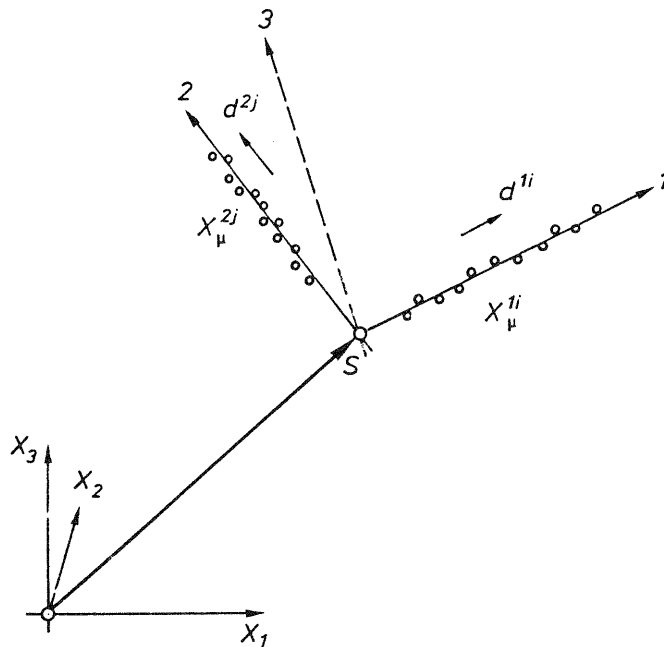
The structure of the program (fig. 3) permits an interactive approach to the multimedia resection problem. By selectively specifying the input data, the operator may repeat the computations as often as he wants. The resection phase is completed when all photographs of the same object are processed.

In the intersection part the orientation parameters and the polynomial coefficients are used for a rigorous spatial intersection of all object points imaged on the photographs. The ray from an image point to its corresponding object point is defined by the position of its intersection with the boundary plane directly adjacent to water in object space ( $P_3$  in fig. 2) and by a unit vector giving its direction. In a first phase the control points are intersected from each pair of photographs, the (spatial) residuals are displayed both numerically and graphically, and the operator again has the option to compensate for certain systematic disturbances not covered previously, e.g. the gradient of refractive index in water. It is possible to utilize a set of trivariate polynomials in a manner analogous to resection. The mean of the results of all processed photopairs is the basis for an error analysis, i.e. a diagram of the final residuals, histogram, RMSE values, etc. If necessary a gross error in one of the control point data may be eliminated. By using the determined trivariate polynomials, all points on the actual object are intersected from each photopair in the second phase. Prior to averaging these object coordinates, however, they have to be further processed according to conditions imposed by the nominal geometry of the particular type of object.

#### GEOMETRIC OBJECT CONDITIONS

The points on the object to be measured are situated on a series of square sleeves of size 250 mm by 250 mm. Together, the sleeves form the skeleton of a rectangular box roughly 5 m in length. Showing two sides of the sleeves only, in the photographs some eight points were measured on either side of a sleeve (see fig. 4). Since each

Figure 4.  
Object geometry



sleeve can be assumed to represent a perfect square within tolerances substantially below the accuracy attainable by photogrammetry, the shape of the object is fully described if, for each sleeve, the spatial coordinates of the corner point S and the orthogonal matrix R defining the orientation of the sleeve with respect to the object base system are given. For the solution adopted, the two sides of a sleeve are considered the axes 1 and 2 (fig. 4) of a spatial Cartesian coordinate system (so-called "fitting system"). If the distances of the estimated points (viz. in total  $m_1$  on 1 and  $m_2$  on 2) from S are denoted by  $d^1$  and  $d^2$ , respectively, then the observation equations are given by ("o" denotes the outer matrix product)

$$\begin{aligned} X^1 + V^1 &= s + d^1 \circ R_{,1} \\ X^2 + V^2 &= s + d^2 \circ R_{,2} \end{aligned} \quad (11)$$

where the  $(m_1, 3)$  and  $(m_2, 3)$  matrices  $X^1$  and  $X^2$ , respectively, are the measured and intersected coordinates and s the coordinates of the corner point. The corresponding linearized system is obtained if three independent rotational parameters, t, are introduced

$$\begin{aligned} X^1 + V^1 &= (I_{m_1} \circ I_3) \cdot s + \left( d^1 \circ \frac{\partial R}{\partial t} \right)_{,1} \cdot dt + (I_{m_1} \circ R_{,1})^{T132} \cdot d^1 \\ X^2 + V^2 &= (I_{m_2} \circ I_3) \cdot s + \left( d^2 \circ \frac{\partial R}{\partial t} \right)_{,2} \cdot dt + (I_{m_2} \circ R_{,2})^{T132} \cdot d^2 \end{aligned} \quad (12)$$

Notice the use of a somewhat extended matrix notation. With  $m = m_1 + m_2$  the system (12) consists of  $3m$  equations and  $6+m$  unknowns. Actually, the system has been solved with an improved stochastic model, viz. with a  $(3, 3)$  weight matrix for the intersected coordinates. The standard errors of the corner point S and the matrix R are substantially smaller or more reliable than for the individual observation points. Finally, the mean from all photopairs has to be computed by rigorous consideration of the individual covariance matrices.

## PROGRAM PACKAGE

In its present state the APL program package consists of four workspaces (WS), viz. *EINLESEN*, *RESEKTION*, *INSEKTION* and *AUSGABE*. These WS are generally considered sufficient for the processing of the photogrammetric data. In addition two more WS were available for the modification, improvement or analysis of the data. All programs and data are available in the Burroughs APL-700 system of the computing center of Munich Bundeswehr University. Program transfer to other APL-systems is possible, although not without considerable modifications.

The intentions have been that each WS consisted of a multitude of preferably small and simple subroutines and functions with as little overlapping as possible. Each WS contains one main routine, called *START*. In order to facilitate any future program changes, it has been considered mandatory to have functionally structured routines not larger than 30 APL lines at the most. This modern philosophy entails a deep-leveled program structure. Due to the high degree of interactivity desired for the final program package, a considerable part consists of "overhead" programming necessary for the entire structure. In fact, from the total number of 1435 APL program lines, only 450 may be attributed to real photogrammetric computations. See also fig. 5

WS	APL program lines	
	photogrammetric	total
<i>EINLESEN</i>	25	140
<i>RESEKTION</i>	125	555
<i>INSEKTION</i>	300	540
<i>AUSGABE</i>	0	200
total:	450	1435

Figure 5. Number of APL-lines

WS *EINLESEN* reads the photogrammetric data of one or several projects from an APL-external file via shared variables into the APL-system and stores it after some preliminary validity checks in a reorganized manner on APL-file. As each photopair has been measured twice, the differences between the two sets of image coordinates larger than a prespecified tolerance limit are used for elimination. In the APL-file only the averaged coordinates are stored. The number of APL-lines is shown in fig. 5.

WS *RESEKTION* has been described in detail in Section 4. Its interactivity part consists mainly of selecting the photopairs to be processed, eliminating gross errors and compensating systematic errors. This is facilitated by various displayed tables and graphs. In order to have an impression of the APL program, the main routine, *START*, together with the functions and variables in the WS are exhibited in the appendix. WS *INSEKTION* has been described in detail in Section 4 as well. It also contains the processing of all points measured on the object. The final results are stored on APL-file. WS *AUSGABE* transfers the data from APL-file back to APL-external file.

## PRELIMINARY TEST RESULTS

To date the method could not yet be tested under water. Preliminary tests were carried out under simulated though normal atmospheric conditions. A dummy test object was photographed in scale 1:36. The standard errors of the sleeve corners ranged between 0.12 and 0.19 mm in X (left to right), 0.06 and 0.11 mm in Y (distance), and 0.04 and 0.07 mm in Z (height). For the outer corner points of the sleeves, standard errors remained between 0.06 and 0.10 mm in X, 0.11 and 0.20 mm in Y, and 0.06 and 0.10 mm in Z. If we consider that the conditions under water ought to be less favorable, standard errors less than 0.5 mm are realistic.

REFERENCES

- DORRER, E. 1982. "Application of APL to Numerical Computations in Analytical Photogrammetry". In: Proc. Math. Models, Accuracy Aspects, and Quality Control, Helsinki, June 7-11; 97-113.
- HOEHLE, J. 1971. "Zur Theorie und Praxis der Unterwasser-Photogrammetrie". DGK, Reihe C, Heft 163, München; 96 p.
- OKAMOTO, A. and HOEHLE, J. 1972. "Allgemeines analytisches Orientierungsverfahren in der Zwei- und Mehrmedien-Photogrammetrie und seine Erprobung". BuL, Jahrg. 40, Heft 2; 103-119.
- RINNER, K. 1948. "Abbildungsgesetz und Orientierungsaufgaben in der Zweimedienphotogrammetrie". Sonderheft 5, Österr. Zeitschrift f. Verm. Wesen, Wien; 46 p
- RINNER, K. 1969. "Problems of Two-Medium Photogrammetry". Phot. Eng. Vol. 35, No. 3; 275-282
- TORLEGARD, A.K.I. 1974. "Under-Water Analytical Systems". Phot. Eng. Vol. 40, No. 3; 287-293
- WESTER-EBBINGHAUS, W. 1983. "Einzelpunkt-Selbstkalibrierung - Ein Beitrag zur Feldkalibrierung von Aufnahmekammern". DGK Reihe C, Nr. 289, München
- ZAAR, K. 1948. "Zweimedienphotogrammetrie". Sonderheft 4, Österr. Zeitschrift f. Verm. Wesen, Wien; 36 p.

APPENDIX

- (A) Fundamental APL application function *SRIM* representing the refracto-collinearity condition.

Arguments:

*X* ... (3)-vector or (m,3)-matrix of spatial coordinates in "housing" system

*ND* ... (g,2)-matrix of refraction parameters (see Section 3)

$$ND \leftrightarrow \begin{matrix} n_1 & d_0 \\ & n_2 & d_1 \\ & & : & : \\ & & & n_g & d_{g-1} \end{matrix}$$

*XR* ... (2)-vector or (m,2)-matrix of normalized "image housing" coordinates

```

∇ SRIM[ ] ∇
∇ XR←ND SRIM X;R;L;H;RH;T;RHO;RX;N
[1] L←00÷(ND←(2+1,ρND)ρND)[;1]
[2] R←(+/(X←((×/RX←1+ρX),3)ρX)[;12]*2)*÷2
[3] RH←T÷00H×1>|H←(00÷N)×T←(R÷-X[;3])×N←ND[1+ρND;1]
[4] H←(((1+ND[;2])○.×N),[1]-X[;3]++/ND[;2])÷ND[;1]○.×H←(ρR)ρ1
[5] IT:RH←R÷ND[1;2]++/[1]H÷40L○.×RHO←RH
[6] →(√/1E-10<|RHO-RH)↑IT
[7] XR←(RX,2)ρ-X[;12]×(RH÷R)○.×2ρ1
∇

```



(B) Functions, variables and main program *START* of WS *RESEKTION*

```
)LOAD RESEKTION
(BVWE10K)RESEKTION ON FBGEOD
SAVED 86/02/27 12.57.45

)FNS
AFTR AFTRΔ0Δ ANZEIGE AUSGABE BERECHNUNG1 BERECHNUNG2 CTR DISTORCO
DOP EINGABEΔA EINGABEΔB EINGABEΔ0 EINGABEΔ1 EINGABEΔ2
EINGABEΔ3 EINGABEΔ4 EINGABEΔ5 EINGABEΔ6 EINLESENΔ1 EINLESENΔ2
EINLESENΔ3 ELIMINATION ELMAT EPS ERGEBNIS ERGEBNISΔ1
ERGEBNISΔ2 ERGEBNISΔ3 FEHLER FRAGE FRAGEKENNZ FRAGEKONFIDENZINT
FRAGEWERTE GINV GLOCKE ID INITIAL KOPF KREIS LENS LIES MEAN
NIM ORTMAT ORTMATΔ ORTMAT_1 PAUSE PETR PETRΔSΔ PETRΔXΔ PLOT
PLOTERGEBNIS POLEST2 POLINT1 POLINT2 POLOPT2 POLSIG2 PROJEST2
PROJETR2 PRUEFEΔE3 PRUEFEΔE4 PRUEFEΔE5 PRUEFEΔKI
REFRACTORESECT3 ROTMAT ROTMAT_1 RUECKFRAGE SKALA SPEICHERN
SRIM SRIMΔNDΔ SRIMΔXΔ START STEUERUNG SYNTAX TEL TE2 TE4
TE5 TST VERARBEITUNGΔA VERARBEITUNGΔB VERARBEITUNGΔC
VERLEGENHEIT1 VORSCHUB ZEICHNEΔ1 ZEICHNEΔ2 ZEIT ZUWEISENΔE4
ZUWEISENΔE5 ZWERGEBNIS ZWERGEBNISΔ1 ZWERGEBNISΔ2 ZWSPEICHERNΔ1
ZWSPEICHERNΔ2 ZWSPEICHERNΔ3

)VARS
AV B BR BU C1S C2S FE F1 F2 F3 HO HP KE LF NDS NR OBJT
OBNA OBWE OR PME3 PME4 PME5 PMKI R SO TEL1 TER3 TE01
TE02 TE1 TE41 TE42 TE51 TE52 TE6 TP TR TR1 TS TST1 TST11
UKU V WS XCP XCR XICP XIPC Z ZD ZR Z1 Z2 Z3 PXOP XIR
XOPC Z ZD ZR

VSTART[[]]V
V START;BILDNR;DATNAM;GERAET;RUECK;T1;T2;T3;ZEILEN;ZZ
[1] EINGABEΔA
[2] L1:EINGABEΔB
[3] VERARBEITUNGΔA
[4] →L1×\FEHLER
[5] L2:ERGEBNIS
[6] →(L1,L2,L3,L4,L6)[STEUERUNG]
[7] L3:ELIMINATION
[8] →L5
[9] L4:VERARBEITUNGΔB
[10] L5:VERARBEITUNGΔC
[11] →(L1×\FEHLER),L2
[12] L6:SPEICHERN
V
```